Proc. Natl. Acad. Sci. USA
Vol. 91, pp. 3829–3833, April 1994
Physiology

Diffusivity of myoglobin in intact skeletal muscle cells

(oxygen transport/facilitated diffusion/photooxidation)

KLAUS D. JÜRGENS*, THOMAS PETERS, AND GEROLF GROS

Zentrum Physiologie, Medizinische Hochschule, 30623 Hanover, Germany

Communicated by Ewald R. Weibel, December 15, 1993 (received for review October 15, 1993)

ABSTRACT **We report a method that allows us to determine the diffusion coefficient of native myoglobin in intact and mechanically unaffected red muscle fibers. The method is based on an optical recording of intracellular diffusion of metmyoglobin, which is produced inside the cells by photooxidation of oxymyoglobin with a UV light pulse. We find a myoglobin diffusivity of 1.2×10^{-7} cm^2/s (22°C), which is only 1/10th of the value measured in very dilute myoglobin solutions and 1/5th of the value obtained from measurements in solutions of myoglobin at 18 g/dl. The latter value often has been used in model calculations of oxygen transport to tissue incorporating myoglobin-facilitated oxygen diffusion. Recalculating facilitated diffusion with the value obtained by us implies that its contribution to total intracellular oxygen transport is of minor importance. Furthermore, it shows that sterical hindrance to myoglobin diffusion is dominated by the muscle-cell architecture rather than by the overall protein concentration of the muscle fiber.**

It is widely accepted that myoglobin serves as an oxygen buffer during temporary deficits in oxygen supply—for instance, as a long-term reservoir during dives of aquatic mammals, in which it occurs in concentrations up to 5 mmol/kg of muscle (1), or as a short-term oxygen store in times of restricted blood perfusion in the beating heart or exercising skeletal muscle of land mammals (2), in which it is found in concentrations up to 0.5 mmol/kg of muscle (1). Another potential role of myoglobin is that it enhances intracellular oxygen diffusion in red skeletal muscle cells by loading oxygen at sites where the Po_2 is high enough to saturate the hemoprotein and releasing the oxygen according to its oxygen-binding properties at sites with low Po_2. Here less agreement is found in the literature as to what extent the flux of oxymyoglobin contributes to the overall oxygen transport within the cell. Experimental (3, 4) and theoretical (5, 6) studies yielded contradictory results. Quantitative statements so far were derived only from model calculations. Such results strongly depend on the value that is used for the mobility of myoglobin inside the muscle cell. Since the actual value of the intracellular diffusion coefficient of native myoglobin (D_{Mb}) has not been determined so far in mammalian skeletal muscle cells, a value obtained from measurements in concentrated (18 g/dl) myoglobin solutions has been used instead.

In general, only little is known about the cytoplasmic mobilities of proteins. Furthermore, the few data available so far for the intracellular diffusion coefficients of proteins were all obtained in artificially altered cells—e.g., in skinned muscle fibers, from injection of labeled molecules into cells, or from fused cells.

We have now developed a method that allows us to measure diffusivities of intracellular hemoproteins without mechanically affecting the cells at all. The method is described, and a result is presented for the intracellular D_{Mb} in intact cells of rat diaphragm muscle. Our value for intracellular D_{Mb} is considerably smaller than expected from the measurements in protein solutions. The consequences arising for myoglobin-facilitated oxygen transport are discussed.

MATERIALS AND METHODS

Muscle Preparation. Male Wistar rats were premedicated with 5000 international units of heparin i.p. per kg of body weight to prevent blood clotting and with 0.2 mg of atropin s.c. and 3 mg of diazepam i.m. per kg for sedation before they were anesthetized with 100 mg of ketamin and 15 mg of xylazin i.p. per kg. One common carotid artery was cannulated and connected to a perfusion system. The abdominal caval vein was opened, and the circulatory system was perfused for 15 min with oxygen-equilibrated Hanks' solution, to which 35 g of dextran, 50 mg of papaverin (for blood vessel dilatation), and 2200 units of heparin were added per liter. The blood-free perfused diaphragm muscle was excised, and an appropriate part of it was mounted into a measuring chamber.

For the purpose of control experiments, *Xenopus laevis* frogs were treated with 1000 units of heparin before being anesthetized by submersion in water containing 0.1 g of tricain methanesulfonate per dl. The truncus arteriosus was cannulated and connected to the perfusing system. The heart ventricular wall was opened, and the animal was perfused for 1 hr with oxygen-equilibrated frog Ringer solution, to which 2200 units of heparin and 50 mg of papaverin were added per liter. Part of the blood-free perfused lateral abdominal wall was excised, and a single muscle layer, prepared from this tissue, was mounted into the measuring chamber.

In the measuring chamber the rat diaphragm muscle was superfused with 95% O_2/5% CO_2-equilibrated Krebs–Henseleit solution (pH 7.4); the frog muscle was superfused with oxygen-equilibrated frog Ringer solution (pH 7.4). At the oxygen partial pressure (Po_2) of around 690 torr (1 torr = 133.3 Pa), which is given by equilibrating the superfusate with 95% O_2/5% CO_2, complete oxygenation of myoglobin was assured throughout the diaphragm sample. At this Po_2 and a resting O_2 consumption of the muscle tissue of 0.5 ml/(min·100 g of tissue), no anoxic region occurs in muscle sheets up to a thickness of 1.8 mm (calculated with the Warburg equation). This is far from the mean thickness of 0.3 mm of the rat diaphragm.

Measuring Setup. The measuring chamber is equipped with quartz glass windows on top and bottom so that the muscle sample can be transluminated. This chamber is placed into a microscope-photometer (Fig. 1), which has two light paths. Ultraviolet light, produced by a superpressure short-arc mercury lamp (Osram HBO 100W/2), is guided through the epi-illuminating light path onto the muscle sample. As has been shown by Demma and Salhany (7), irradiation with UV light leads to photooxidation of oxygenated hemoproteins,

The publication costs of this article were defrayed in part by page charge payment. This article must therefore be hereby marked "*advertisement*" in accordance with 18 U.S.C. §1734 solely to indicate this fact.

*To whom reprint requests should be addressed.

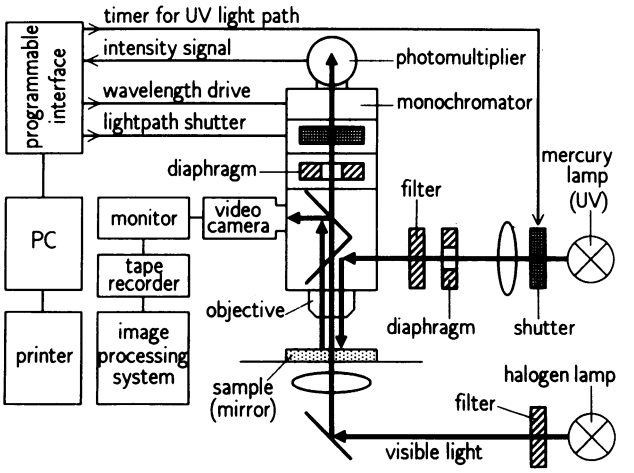

FIG. 1. Scheme of the experimental setup.

and, therefore, in this experimental setup converts part of the cellular oxymyoglobin into metmyoglobin. Fig. 2 shows the light absorbance spectrum in the Soret band of a myoglobin-containing muscle fiber before (curve a) and after (curve b) UV irradiation. The absorbance peak is shifted to shorter wavelengths, which results in a considerable decrease in absorbance at a wavelength of 420 nm, where the absorbance coefficients of oxy- and metmyoglobin are markedly different. A UV pulse of 2-s duration oxidizes between 5% and 15% of the cellular oxymyoglobin. No significant absorbance change is observed when muscle fibers of a deoxygenated sample (curve c) are subjected to such an UV exposure (curve d).

Fig. 3 *Inset* shows the geometry of the UV-irradiated area on the muscle sample, which is given by an adjustable rectangular optical diaphragm in the UV light path. In the y direction, this field extends over a few fibers; in the x direction—i.e., in the direction of the fiber axes—the field width (w) ranges between 70 and 500 μm. By the UV light pulse, a concentration gradient of metmyoglobin is generated between the irradiated field and its surroundings, causing metmyoglobin to diffuse out of and oxymyoglobin to diffuse into this field along the fiber axis. The disappearance of metmyoglobin from a narrow measuring field in the center of the irradiated field (see Fig. 3 *Inset*) is observed by means of the second light path. Visible light of a halogen lamp transluminates the sample, and its intensity at 420 nm, which strongly depends on the ligation state of the cellular myoglobin, is measured by the photometer (Fig. 1).

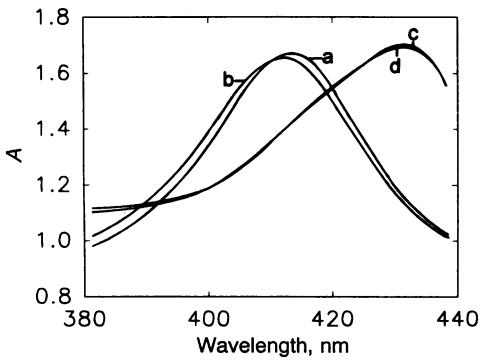

FIG. 2. Absorbance spectrum of myoglobin-containing diaphragm muscle fibers in the oxygenated state (curve a) after partial formation of metmyoglobin by UV light (curve b) and in the deoxygenated state before (curve c) and after (curve d) UV exposure.

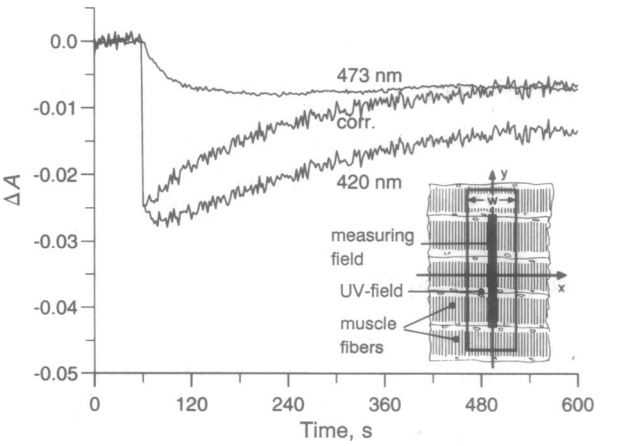

FIG. 3. Absorbance change due to photooxidation of myoglobin and subsequent metmyoglobin diffusion/reduction kinetics. Original recordings at 420 nm and 473 nm are shown as well as the corrected kinetics. (*Inset*) Arrangement of UV-irradiated field and measuring field on the muscle sample. The width w is varied between 70 and 500 μm.

The absorbance is calculated from the ratio of the light intensity signals given by the muscle sample and a reference sample. The reference signal was obtained from an area in the tendinous center of the diaphragm. The whole measuring procedure is performed by a computer program, running on a personal computer supported by a programmable interface.

Fig. 3 gives an example of the formation of metmyoglobin due to the UV light pulse (the abrupt fall in absorbance) and the time course of the subsequent disappearance of the oxidized hemoprotein from the measuring field recorded at 420 nm.

The duration of the exposure time and the wavelength range of the applied UV light were carefully selected to avoid any damage of the muscle cells. In all of the evaluated experiments, no microscopically visible alterations of the fibers could be observed during the measuring period. Nevertheless, small invisible side effects of the irradiation did occur and influenced the signal of the metmyoglobin kinetics. This was revealed by simultaneously recording the time course of the signal at 473 nm (Fig. 3), an isosbestic wavelength for oxy- and metmyoglobin. Control experiments with sheets of the myoglobin-free abdominal oblique muscle of the frog *Xenopus laevis* showed that this side effect has the same magnitude and the same time course at both 420- and 473-nm wavelengths (see Fig. 4). Therefore, it is justified to subtract the 473-nm signal from the 420-nm signal to obtain the correct myoglobin kinetics (corrected in Fig. 3). The side effect is possibly due to damage of transport proteins in the membranes by UV light, followed by a slight water uptake of the cells.

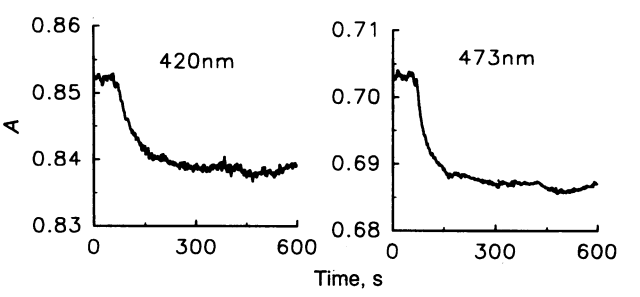

FIG. 4. Time course of the absorbance changes simultaneously recorded at 420 and 473 nm in myoglobin-free frog abdominal muscle after a 4-s UV exposure.

Mathematical Description of the Problem. The disappearance of metmyoglobin from the irradiated area is not exclusively due to myoglobin diffusion but also can be caused by metmyoglobin reductase activity. This effect has been taken into account by assuming first-order kinetics in the differential equation describing the process:

$$\frac{dC_{Mb}}{dt} = D_{Mb}\frac{d^2C_{Mb}}{dx^2} - k_{Mb}C_{Mb}, \quad [1]$$

where C_{Mb} is the metmyoglobin concentration after the UV exposure and k_{Mb} is the reaction rate constant of the enzymatic reduction. If one assumes validity of Beer's law, C_{Mb} is related to the measured absorbance change ΔA by the equation

$$\Delta A = C_{Mb}\,(\varepsilon_{met} - \varepsilon_{oxy})\,d, \quad [2]$$

where ε is the absorbance coefficient of met- and oxymyoglobin, respectively, and d is the thickness of the muscle sample. Inserting this relation into the previous one leads to

$$\frac{d(\Delta A)}{dt} = D_{Mb}\frac{d^2(\Delta A)}{dx^2} - k_{Mb}(\Delta A). \quad [3]$$

This differential equation can be solved numerically with the Crank–Nicolson algorithm provided that the respective boundary and initial conditions are known.

In this respect it is of importance to note that within the irradiated field of each muscle fiber, the focused light beam of the mercury lamp generates a constant UV intensity in the y direction, but, mainly at larger field widths, the intensity varies along the x coordinate. The absorbance profile along the x axis immediately after exposing the sample to this UV light intensity distribution represents the initial condition that has to be known to solve the differential equation. We have shown for a given exposure time (which is <2 s) that the corresponding initial change in absorbance ΔA_0, measured in the center (at $x = 0$) of the irradiated field of the diaphragm muscle, is proportional to the applied UV light intensity (Fig. 5). Furthermore, in a model system consisting of agar gels impregnated with hemoglobin, we could show that such a linear relation between light intensity and initial concentration of the oxidized hemoprotein holds at any site along the x axis within the irradiated area. These measurements were done by video recordings of the irradiated fields and subsequent computerized image processing (see Fig. 1), a direct method that unfortunately was not sensitive enough to be applicable to muscle samples. Therefore, in muscle tissue we indirectly determined the initial distribution of metmyoglobin concentration or the corresponding distribution of absorbance, respectively, by recording the UV light intensity distribution in the plane of the muscle sample with the video system. For each setting of the field width w, such a recording was performed after placing a mirror into the microscope in the plane of the sample.

The solution of the differential equation obtained for the respective initial condition was then fitted to the corresponding measured time course of ΔA with a least-squares method [program E04FDF of the Numerical Algorithms Group (NAG)] library by varying the values of D_{Mb} and k_{Mb}.

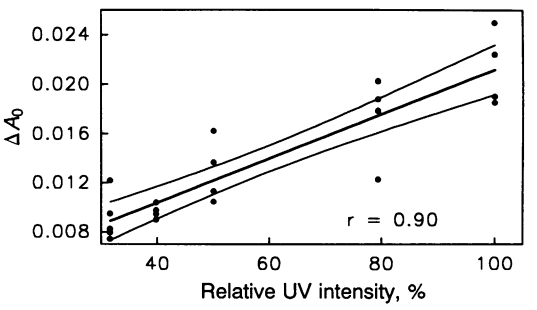

FIG. 5. Absorbance drop ΔA_0 as a function of relative UV light intensity recorded in the center of the UV field immediately after a short UV exposure. Intensities <100% were obtained by inserting calibrated grey filters into the UV light path. Given is the linear regression line and its 95% confidence interval.

RESULTS

Fig. 6 shows measured curves and the corresponding best fits for three different field widths. As expected for a diffusion process, the disappearance of metmyoglobin from the center of the irradiated field becomes faster as the chosen width of the irradiated field becomes smaller.

From 76 measurements, recorded from the diaphragm muscles of six male Wistar rats at field widths between 71 and 497 μm, we obtained at 22°C for intracellular D_{Mb} a value of $(1.17 \pm 0.08)10^{-7}$ cm^2/s and for k_{Mb} a value of $(1.48 \pm 0.20)10^{-3}$ s^{-1} (both are means ± SEM). Since the width of the irradiated field influences the diffusion kinetics but not the reaction kinetics of metmyoglobin, the wide range of applied field widths (10 different values of w) was favorable for discriminating between the influence of k_{Mb} and D_{Mb} on the kinetics. At a field width of 71 μm, the decrease of metmyoglobin to half of its initial concentration is caused ≈80% by diffusion and ≈20% by enzymatic reduction. At a field width of 284 μm, the corresponding drop is caused ≈20% by diffusion and ≈80% by reduction.

DISCUSSION

The mean value obtained for the reduction rate constant k_{Mb} is in good agreement with data of Hagler *et al.* (8), who found a value of 1.1×10^{-3} s^{-1} at 22°C in the soleus muscle of the rat. These authors also demonstrated a positive correlation between myoglobin reductase activity and myoglobin content in different muscles, a fact that may explain the markedly lower value of k_{Mb} found by Baylor and Pape (0.27×10^{-3} s^{-1} at 20°C) after injection of metmyoglobin into (normally myoglobin-free) frog muscles (9).

Table 1 shows a comparison of the diffusion coefficient of myoglobin determined by the UV method with other protein diffusion coefficients, measured in axial or radial direction of muscle cells as well as in highly concentrated myoglobin

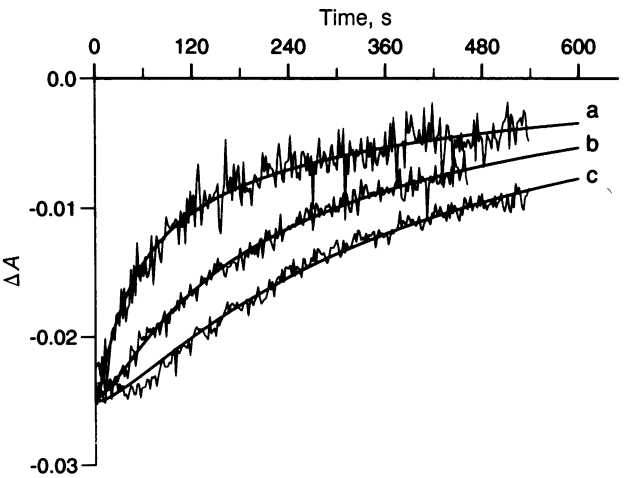

FIG. 6. Measured absorbance changes after photooxidation and their best fits given for three widths of the irradiated field: 71 μm (trace a), 142 μm (trace b), and 284 μm (trace c).

Table 1. Protein diffusion coefficients in skeletal muscles and in solutions (37°C)

Protein (kDa)	Sample	D, cm²/s	D/D_0	Ref.
Myoglobin (17.2)	Rat diaphragm (UV method), axial	1.7×10^{-7}	0.10	This work
	Frog muscle (injection), axial	2.4×10^{-7}	0.14	9
	Rat muscle, homogenate	2.7×10^{-7}	0.16	10
	Solution (18 g/dl)	8.1×10^{-7}	0.47	11
	Solution (24 g/dl)	5.5×10^{-7}	0.32	11
Parvalbumin (11)	Skinned frog muscle, radial	2.5×10^{-7}	0.15	12
TPI (53)		0.75×10^{-7}	0.08	12
PGM (66)		0.70×10^{-7}	0.08	12
G3PD (144)		0.37×10^{-7}	0.05	12

Diffusion coefficients of myoglobin obtained from measurements in muscle cells, in muscle homogenate and in concentrated myoglobin solutions. For comparison, diffusion coefficients of other proteins obtained from measurements in skinned frog muscle fibers are shown. D/D_0 denotes the ratio of the given diffusion coefficients and their corresponding values holding for dilute aqueous solutions. TPI, triose-phosphate isomerase; PGM, phosphoglyceromutase; G3PD, glycerol-3-phosphate dehydrogenase.

solutions. All values are converted to 37°C by applying a Q_{10} (factor by which the diffusion coefficient is increased for a rise in temperature of 10 degrees) of 1.3. This Q_{10} holds for the viscosity change of water, and it is close to the value of 1.4, which has been obtained for myoglobin diffusion in muscle homogenates by Moll (10).

As can be seen in column 4 of Table 1, the ratio of our intracellular value for D_{Mb} to the one measured in highly diluted aqueous myoglobin solutions (D/D_0) is 1/10. It is only one-fifth of the value obtained from measurements of the self-diffusion coefficient in concentrated (18 g/dl) myoglobin solutions (11), a value that is often applied in model calculations involving myoglobin-facilitated oxygen diffusion. Even at a myoglobin concentration of 24 g/dl, which corresponds to the total intracellular protein concentration in muscle cells if both soluble and structural proteins are taken into account, the self-diffusion coefficient of myoglobin is still 3 times larger than the intracellular diffusivity measured here. Therefore, it can be concluded that the axial mobility of proteins in muscle cells is not solely determined by cytoplasmic viscosity but seems to be strongly affected by structural obstacles within the cell.

Our result for intracellular D_{Mb} is supported by experimental findings of Baylor and Pape (9), who measured a 1.4 times higher value after injection of metmyoglobin into frog muscle fibers, and by data of Moll (10), who determined a 1.6 times larger value in homogenates of red muscles. Both authors considered their result an upper limit for intracellular D_{Mb}.

Similar to what we find for the axial diffusion of myoglobin, the intracellular diffusion of proteins in the radial direction has been reported to be reduced to 15% to 5% of the values found in dilute solutions. This has been shown for several proteins in the weight range between 10 and 140 kDa in skinned muscle fibers (12). For parvalbumin (12 kDa), for instance, a reduction of the radial diffusion coefficient to 15% was observed, which is comparable to the axial reduction to 10% measured for myoglobin (17 kDa). These results strongly suggest that similar values of the diffusion coefficient hold for axial and radial diffusion of a protein in muscle cells.

In living amoebae, whose cytoplasm is less structured compared with that of muscle cells, intracellular diffusion coefficients have been determined by injection of fluorescently labeled proteins. Here the reduction of protein diffusivity is considerably smaller than in muscle cells; for ribonuclease (14 kDa), values were reported that range between one-third and one-half of the value found in dilute aqueous solutions (13).

The literature data used in model calculations to estimate the influence of myoglobin-facilitated oxygen diffusion on the oxygen supply of muscle tissue all range between 5×10^{-7} (6) and 18.6×10^{-7} cm²/s (14) and are obviously much too large. This led to an overestimation of the role of facilitated oxygen transport. Therefore, we recalculated the contribution of myoglobin-facilitated oxygen diffusion by the equation derived for the ratio of facilitated diffusion ($\dot{V}O_{2Mb}$) to free oxygen diffusion ($\dot{V}O_{2free}$). This relation is obtained by dividing the equation for the diffusion of oxymyoglobin across a plane sheet by the corresponding equation holding for free oxygen diffusion. On one side of the sheet an O_2 pressure head Po_{2cb} (cell boundary) is given, on the other side the Po_2 is assumed to be zero. Taking into account the law of mass action for the reaction of myoglobin with oxygen, one obtains the following relation:

$$\frac{\dot{V}O_{2Mb}}{\dot{V}O_{2free}} = \frac{D_{Mb}\, C_{Mbtot}}{K_0(Po_{2cb} + P_{50})}. \quad [4]$$

Since the geometrical factors of the two diffusional processes cancel out, Eq. 4 is independent of the assumed geometrical arrangement and, therefore, holds also for other geometrical models than plane sheets.

In Eq. 4 C_{Mbtot} is the total myoglobin concentration, K_0 is Krogh's diffusion constant for free oxygen diffusion in muscle tissue and P_{50} is the oxygen half-saturation pressure of myoglobin.

We found the myoglobin concentration in the cell water of the rat diaphragm to be up to 300 μM. For this myoglobin concentration, the diffusion coefficient determined by us, the K_0 value for rat diaphragm muscle of 0.76×10^{-12} mol/(cm·min·torr) found by Visschedijk (cited in ref. 15), and two different P_{50} values, the curves described by Eq. 4, are given in Fig. 7. In the literature a value of 2.3 torr is reported for

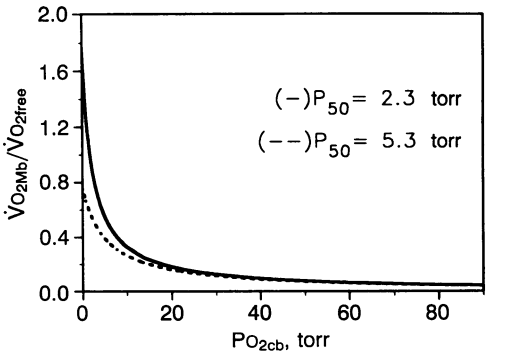

FIG. 7. Ratio of facilitated and free intracellular oxygen flux as a function of a given oxygen partial pressure head at the cell boundary. Shown are the curves for two different oxygen half-saturation pressures of myoglobin.

horse myoglobin P_{50} (16) and a value of 5.3 torr is reported for dog myoglobin (17). Within this P_{50} range, facilitated oxygen diffusion amounts to only 20% to 30% of free oxygen diffusion in the range of Po_{2cb} values between 15 and 10 torr, which may represent the lower limit for a sufficient oxygen delivery to mitochondria at maximal oxygen consumption (18). Even at Po_{2cb} values approaching zero (i.e., at cell anoxia!), where the flux ratio reaches its maximal value, the contribution of facilitated O_2 diffusion amounts to only 80% of the free oxygen diffusion if the P_{50} of myoglobin is 5.3 torr and amounts to 180% if the P_{50} is 2.3 torr.

In a recent paper Bentley *et al.* (19) reported a 3.3 times larger value of K_0 for mammalian striated muscle (retractor muscle of the hamster) than that applied in the above calculations. Inserting this value into Eq. 4 would lead to a further reduction by 70% of the ratio of facilitated to free oxygen diffusion shown in Fig. 7.

In other words, with an intracellular D_{Mb} as measured by us and at myoglobin concentrations as found in red skeletal muscle of land mammals (<0.5 mM), myoglobin-facilitated oxygen diffusion presumably plays only a minor role for muscular oxygen supply.

This statement is underlined by the model calculation shown in Table 2. The Krogh cylinder model for tissue oxygenation is applied to calculate the minimal Po_2 value required at the cell boundary to meet a given oxygen demand. Under resting conditions, with or without facilitated diffusion, very low Po_2 values are sufficient. At an oxygen consumption of 5 ml/(min·100 g of tissue), measured at maximal aerobic performance of human forearm muscles (20), facilitated oxygen diffusion reduces the required Po_2 by only 3.5 torr if our intracellular diffusion coefficient is used. In contrast, a considerable reduction by 13.3 torr is calculated on the basis of the literature D_{Mb} value holding for concentrated (18 g/dl) myoglobin solutions. A similar difference is found for an extremely high maximal oxygen consumption, such as the 16 ml/(min·100 g of tissue) reported by Gayeski *et al.* (17) for the dog gracilis muscle.

Table 2. Po_2 values calculated with the Krogh-cylinder model

Oxygen-consumption, ml/(min·100 g)	Po_{2nfd}, torr	$Po_{2fd1.7}$, torr	Po_{2fd8}, torr
0.5 (rest)	1.9	0.8	0.2
5.0	18.6	15.1	5.3
16.0	59.5	55.6	41.6

Po_2 values required to meet given oxygen demands, calculated from the Krogh-cylinder model. Po_{2nfd}, values estimated without facilitated diffusion; $Po_{2fd1.7}$, values estimated with facilitated diffusion at $D_{Mb} = 1.7 \times 10^{-7}$ cm²/s; and Po_{2fd8}, values with facilitated diffusion at $D_{Mb} = 8 \times 10^{-7}$ cm²/s. Other model parameters used were as follows: $R_{cyl} = 25$ μm, $r_{cap} = 2$ μm, $C_{Mbtot} = 300$ μmol/liter, $P_{50} = 2.3$ torr, $K_0 = 0.76 \times 10^{-12}$ mol/(cm·min·torr), and $Po_2 = 0$ at outer surface of the cylinder.

The reduction of the required Po_2 values due to facilitated diffusion would be even smaller, if the K_0 value of Bentley *et al.* (19) is used in the Krogh-model calculations.

Our calculations suggest that most statements on intracellular oxygen transport in muscle derived so far from more complex mathematical models similarly overestimate the functional role of myoglobin-facilitated oxygen diffusion, since they are all based on too large values of D_{Mb}. From our results it can be concluded that myoglobin-facilitated oxygen diffusion is of minor importance for oxygen supply of muscle tissue. Other functional roles, such as storage of oxygen or a myoglobin-mediated oxidative phosphorylation, as postulated by Wittenberg and coworkers (21), could be of greater significance.

This report is dedicated to Prof. Waldemar Moll on the occasion of his 60th birthday. We thank Diplomate in Mathematics G. Günther-Jürgens for her help in writing and running the computer programs. We further thank Dr. V. Schwarzmann from Zeiss Germany for his help in developing the basic optical assembly of the experimental setup. This work was supported by Grant Gr 489/5 of the Deutsche Forschungsgemeinschaft.

1. Wittenberg, J. B. (1970) *Physiol. Rev.* **50**, 559–636.
2. Millikan, G. A. (1937) *Proc. R. Soc. London B* **123**, 218–241.
3. Wittenberg, B. A., Wittenberg, J. B. & Caldwell, P. R. B. (1975) *J. Biol. Chem.* **250**, 9038–9043.
4. Jones, D. P. & Kennedy, F. G. (1982) *Biochem. Biophys. Res. Commun.* **105**, 419–424.
5. Loiselle, D. S. (1987) *Biophys. J.* **51**, 905–913.
6. Groebe, K. & Thews, G. (1990) *Am. J. Physiol.* **259**, H84–H92.
7. Demma, L. S. & Salhany, J. M. (1977) *J. Biol. Chem.* **252**, 1226–1230.
8. Hagler, L., Coppes, R. I., Askew, E. W., Hecker, A. L. & Herman, R. H. (1980) *J. Lab. Clin. Med.* **95**, 222–230.
9. Baylor, S. M. & Pape, P. C. (1988) *J. Physiol.* **406**, 247–275.
10. Moll, W. (1968) *Pflügers Arch.* **299**, 247–251.
11. Riveros-Moreno, V. & Wittenberg, J. B. (1972) *J. Biol. Chem.* **247**, 895–901.
12. Maughan, D. & Lord, C. (1988) *Adv. Exp. Med. Biol.* **226**, 75–84.
13. Wang, Y., Lanni, F., McNeil, P. L., Ware, B. R. & Lansing-Taylor, D. (1982) *Proc. Natl. Acad. Sci. USA* **79**, 4660–4664.
14. Murray, J. D. (1977) in *Myoglobin*, eds. Schneck, A. G. & Vandecasserie, C. (Univ. Bruxelles, Brussels), pp. 179–201.
15. Kawashiro, T., Nüsse, W. & Scheid, P. (1975) *Pflügers Arch.* **359**, 231–251.
16. Antonini, E. & Brunori, M. (1971) *Hemoglobin and Myoglobin in Their Reactions with Ligands* (North-Holland, Amsterdam), p. 220.
17. Gayeski, T. E. J. & Honig, C. R. (1988) *Am. J. Physiol.* **254**, H1179–H1186.
18. Bylund-Fellenius, A. C., Walker, P. M., Elander, A., Holm, S., Holm, J. & Schersten, T. (1981) *Biochem. J.* **200**, 247–255.
19. Bentley, T. B., Meng, H. & Pittman, R. N. (1993) *Am. J. Physiol.* **264**, H1825–H1830.
20. Hartling, O. J., Kelbaek, H., Gjorup, T., Schibye, B., Klausen, K. & Trap-Jensen, J. (1989) *Eur. J. Appl. Physiol.* **58**, 466–470.
21. Doeller, J. E. & Wittenberg, B. A. (1991) *Am. J. Physiol.* **261**, H53–H62.